Geoscience Frontiers xxx (xxxx) xxx

HOSTED BY

ELSEVIER

Contents lists available at ScienceDirect

China University of Geosciences (Beijing)

Geoscience Frontiers

journal homepage: www.elsevier.com/locate/gsf

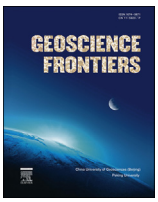

Research Paper

Proto-Adamastor ocean crust (920 Ma) described in Brasiliano Orogen from coetaneous zircon and tourmaline

Léo A. Hartmann [a,*], Mariana Werle [a], Cassiana R.L. Michelin [a], Cristiano Lana [b], Gláucia N. Queiroga [b], Marco P. Castro [b], Karine R. Arena [a]

[a] Instituto de Geociências, Universidade Federal do Rio Grande do Sul, Avenida Bento Gonçalves, 9500, 91501-970, Porto Alegre, Rio Grande do Sul, Brazil
[b] Departamento de Geologia, Escola de Minas, Universidade Federal de Ouro Preto, Morro do Cruzeiro, 35400-000, Ouro Preto, Minas Gerais, Brazil

ARTICLE INFO

Article history:
Received 25 March 2018
Received in revised form
27 June 2018
Accepted 18 September 2018
Available online xxx
Handling Editor: R. Damian Nance

Keywords:
Coeval zircon and tourmaline
Bossoroca ophiolite
Early Brasiliano Orogen
Zircon U-Pb-Hf isotopes
Zircon trace elements
Tourmaline boron isotopes

ABSTRACT

Proto-Adamastor ocean bathed Rodinia and successor continental fragments from 1.0–0.9 Ga up to 0.75 Ga, and evolved into world Adamastor Ocean at 0.75–0.60 Ga. Mesoproterozoic oceanic crust is poorly preserved on continents, only indirect evidence registered in Brasiliano Orogen. We report first evidence of ophiolite originated in proto-Adamastor. We use multi-technique U-Pb-Hf zircon and $\delta^{11}B$ tourmaline isotopic and elemental compositions. The host tourmalinite is enclosed in metaserpentinite, both belonging to the Bossoroca ophiolite. Zircon is 920 Ma-old, $\varepsilon_{Hf(920\ Ma)} = +12$, $Hf_{TDM} = 1.0$ Ga and has 'oceanic' composition (e.g., U/Yb < 0.1). Tourmaline is dravite with $\delta^{11}B = +1.8‰$ (Tur 1), 0‰ (Tur 2), −8.5‰ (Tur 3). These characteristics are a novel contribution to Rodinia and associated world ocean, because a fragment of proto-Adamastor oceanic crust and mantle evolved at the beginning of the Brasiliano Orogen.

1. Introduction

Proto-Adamastor was a narrow ocean that bathed internally fragmented Supercontinent Rodinia in the Mesoproterozoic–Neoproterozoic transition (1.2–0.9 Ga, extending to 750 Ma). Oceanic crust formed between spreading continental fragments of Rodinia until reassembly into Gondwana. World Adamastor Ocean paired Gondwana continental fragments (750–600 Ma). This concept of supercontinent cycle is well established (e.g., Nance and Murphy, 2013), but Rodinia and coeval oceanic crust and mantle are poorly preserved in the extensive continental tracts. Poor characterization of initial oceans led to various names related to Rodinia, including Panthalassa, Mirovoi (e.g., Cawood et al., 2016), Iapetus, Charrua, so we prefer the usage of proto-Adamastor Ocean.

The significance of the Brasiliano Orogen for continental construction in the Neoproterozoic–Cambrian is comparable to the Himalayas in the last 60 Ma. The orogen extends for 4000 km from northeastern Brazil to northeastern Argentina, and for 1500 km from the Atlantic Ocean coast to west-central Brazil as part of the Brazilian Shield (Hartmann and Delgado, 2001). This orogen registers the first manifestation of Rodinia supercontinent breakup in ophiolites, as envisaged by Li et al. (2008), Bogdanova et al. (2009) and Nance and Murphy (2013) for the general process. A review of Brazilian remnants of oceanic crust was published by Suita et al. (2004). All evidence for proto-Adamastor and Adamastor in this extensive orogen is indirect (e.g., Basei et al., 2018) and restricted to granitic (Queiroga et al., 2007) and gneissic rocks and to common, remnant zircon crystals in magmatic, sedimentary, and metamorphic rocks. Adamastor oceanic crust is registered in similar rock associations, and direct evidence was identified in ophiolites by Arena et al. (2016, 2017, 2018a, b). A suggestion of mid-ocean ridge is made in some paleo-continent reconstructions (Fig. 1a), making significant any finding of direct evidence of oceanic crust in the early Tonian.

Direct dating of oceanic crust and mantle in the Brasiliano Orogen is hampered by the low-U content (commonly no zircon) of rocks in ophiolites. A step forward is the identification of zircon from altered oceanic crust rocks and application to Gondwana amalgamation by Arena et al. (2016, 2017, 2018a). A significant comparison resides in the Central Eastern Desert of Egypt, where

* Corresponding author.
E-mail address: leo.hartmann@ufrgs.br (L.A. Hartmann).
Peer-review under responsibility of China University of Geosciences (Beijing).

https://doi.org/10.1016/j.gsf.2018.09.018

Please cite this article as: Hartmann, L.A et al., Proto-Adamastor ocean crust (920 Ma) described in Brasiliano Orogen from coetaneous zircon and tourmaline, Geoscience Frontiers, https://doi.org/10.1016/j.gsf.2018.09.018

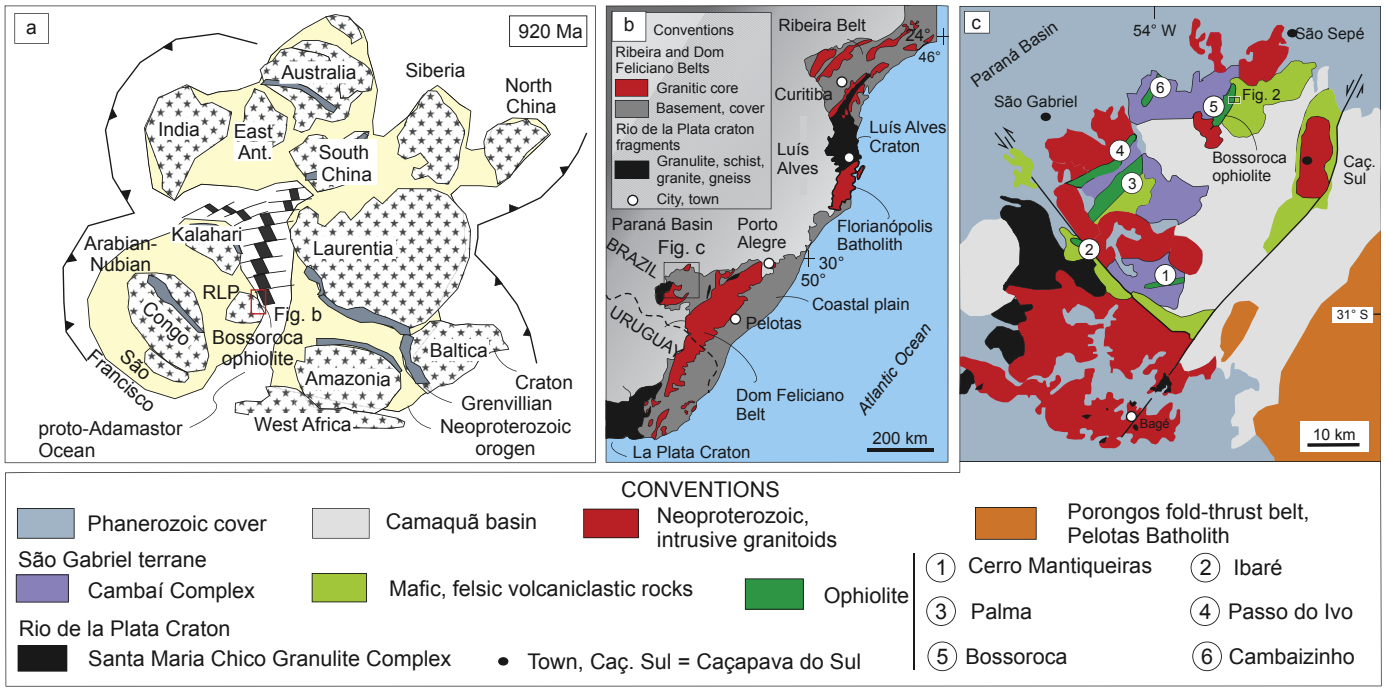

Figure 1. (a) Study area in Rodinia; configuration of Rodinia at 920 Ma (modified from Li et al., 2008; Bogdanova et al., 2009); location of Bossoroca ophiolite and Fig. 1b indicated; (b) Geological map of southern Brazilian Shield; location of Fig. 1c indicated; from Arena et al. (2016); (c) Geological map of São Gabriel terrane and fragments of Rio de La Plata Craton; location of Bossoroca ophiolite and Fig. 2 indicated (from Arena et al., 2016).

the oldest documented units are ensimatic assemblages, with ~750 Ma U-Pb zircon ages (Stern, 2018).

We presently advance description of proto-Adamastor oceanic crust by reporting U-Pb-Hf zircon and δ^{11}B tourmaline isotopic and elemental investigation in a tourmalinite from the Bossoroca ophiolite (920.4 ± 9.8 Ma) in southern Brasiliano Orogen. This age was foreseen by Brito-Neves et al. (1999) within a time span of rifting of Rodinia in the continent (1000–900 Ma). Tourmaline is dravite and zircon has 'oceanic' composition, $\varepsilon_{Hf(920\ Ma)} = +12$ and Hf_{TDM} = 1.0 Ga. Dravite from this Bossoroca tourmalinite has $\delta^{11}B = +1.8‰$ (Tur 1), 0‰ (Tur 2), −8.5‰ (Tur 3). This is a novel contribution to Rodinia and associated world ocean by reporting evidence of a fragment of proto-Adamastor oceanic crust and mantle in the Brasiliano Orogen. The Bossoroca ophiolite is a remnant of altered oceanic crust and contributes to unraveling proto-Adamastor world-ocean evolution.

2. Geological controls

Ophiolites from the Sul-Riograndense Shield (Fig. 1b) are abundant in the São Gabriel terrane (Arena et al., 2016, 2017, 2018a; Philipp et al., 2018) but also occur in eastern Pelotas Batholith (Ramos et al., 2018) and intervening Porongos fold and thrust belt (Pertille et al., 2018; Arena et al., 2018a). Their distribution is thus comparable to other collisional orogens, e.g., Alps, because ophiolites occur in sutures but also thrusted long distances (100–300 km) from the suture.

The Bossoroca ophiolite extends for 20 km NE and has a width of 2 km (Fig. 1c), dipping 60°–80° to NNW. The ophiolite was covered tectonically by Cambaí Complex TTG rocks on the west and was obducted during the Neoproterozoic onto the Campestre Formation volcanoclastic rocks to the east. The main foliation is low-amphibolite facies, NNE-directed, dipping steeply to NW;

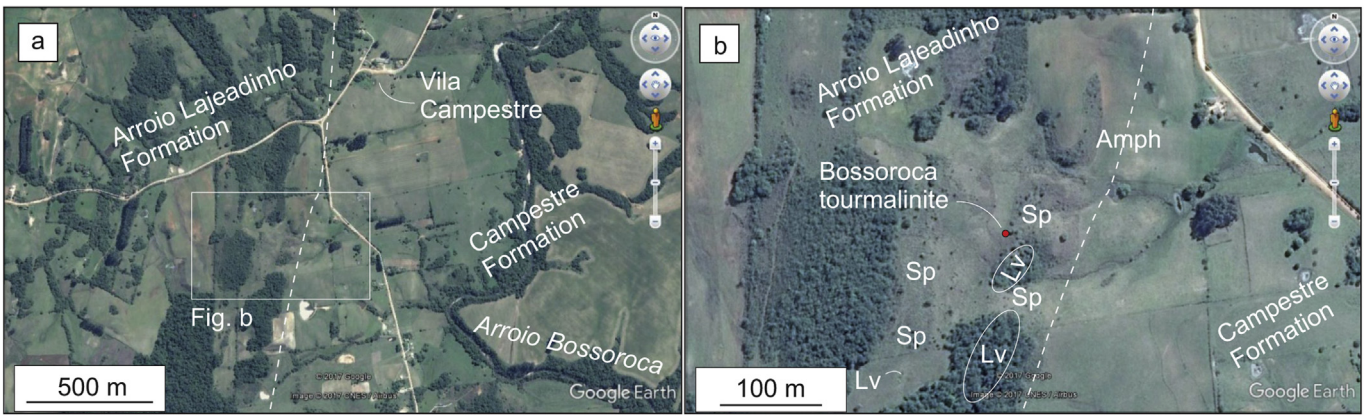

Figure 2. Satellite images of the region of occurrence of Bossoroca tourmalinite; white broken line indicates approximate contact of Arroio Lajeadinho and Campestre formations. (a) Regional view; (b) Detailed view of tourmalinite geological environment. Sp = serpentinite, Lv = listvenite, Amph – amphibolite.

Please cite this article as: Hartmann, L.A et al., Proto-Adamastor ocean crust (920 Ma) described in Brasiliano Orogen from coetaneous zircon and tourmaline, Geoscience Frontiers, https://doi.org/10.1016/j.gsf.2018.09.018

the foliation corresponds to D2 of Saalmann et al. (2006, 2007), marking the obduction of the ophiolite into and over an oceanic arc. D3 was transcurrent faulting, whereas D4 was local thrusting. Older Rio de La Plata Craton rocks are present below the juvenile terrane, because of isotopic composition of young granites, leading to the identification of a metacraton in the region (Santos et al., 2019).

The ophiolite is included in the Arroio Lajeadinho Formation, which makes up the Bossoroca Complex when added to the Campestre Formation (Hartmann et al., 2011). This stratigraphic nomenclature (Supplementary File 1) is well established (Koppe et al., 1985; Saalmann et al., 2007; Lena et al., 2014), although stratigraphy of intermingled ophiolite and oceanic arc is inherently complex leading to different proposals (e.g., Gubert et al., 2016; Philipp et al., 2018).

The mantle section of the ophiolite is made up of numerous serpentinites (50–500 m) with olivine + talc + chromite, associated with the stratiform Mata Grande gabbro (mafic-ultramafic complex) and amphibolite (plagioclase + hornblende), in addition to numerous, irregular metachert layers. Listvenite occurs as 20–200 m long and 2–100 m thick, massive bodies, displaying accessory chromite. Many layers of serpentinite and metachert were deformed into sigmoidal blocks during deformation related to NE-oriented, pervasive shear zones. The shears are interpreted as related to ophiolite obduction into the island arc.

The presence of the assemblages of metamorphic olivine + talc (jackstraw texture) in metaserpentinite and plagioclase + hornblende (EPMA analyses; Koppe and Hartmann, 1990; Remus et al., 1999) in amphibolite sets the metamorphic grade at low amphibolite facies. Listvenite commonly forms in low amphibolite facies by metasomatic alteration of ocean-floor rocks.

The studied tourmalinite is massive, 1 m × 1 m × 1 m, enclosed in metaserpentinite and close (50 m) to amphibolite and listvenite (Fig. 2). The outcrop is located at coordinates 235540 E, 6640705 N, zone 22J, reference system WGS 84. The occurrence is named 'Bossoroca tourmalinite' for the host ophiolite and proximity to Bossoroca gold mine. Color of rock is nearly black, tourmaline crystals up to 10 cm in length constituting 90 vol.%, significant volume of chlorite and minor zircon.

Granitic rocks intrusive into the ophiolite and associated oceanic arc are the São Sepé Granite, located 10 km to NE of the studied area and the Ramada Granite 10 km to south, ages approximately 550 Ma.

3. Methodology

Observation of satellite images and aeromagnetometric and aerogammaspectrometric maps was followed by field work in the Bossoroca ophiolite, culmination of several decades of field observations and laboratory studies. One block of tourmalinite was encountered after two days of search in the bushes and high grasses of the region previously known to contain some blocks of this rare rock type. The rock was described and sampled for laboratory studies. Thin sections and polished mounts of tourmalinite were studied with optical and scanning electron microscopy at Laboratório de Geologia Isotópica, Universidade Federal do Rio Grande do Sul. Backscattered electron images and EDS analyses were used to guide spot analyses, in a similar procedure as used afterwards in the Departamento de Geologia, Universidade Federal de Ouro Preto, Minas Gerais. At UFOP, several analytical techniques were used in both zircon and tourmaline, including chlorite. The presence of zircon included in tourmaline led to specific studies of the mineral, both in polished thin section and mineral separations mounted in epoxy. The techniques included electron microprobe analyses and backscatered electron imaging, followed by U-Pb-Hf-trace element determinations with a laser. Zircon crystals were first analyzed for trace elements, followed by U-Pb isotopes and then Lu-Hf isotopes; BSE imaging guided the positioning of the spot that was placed as close as possible in

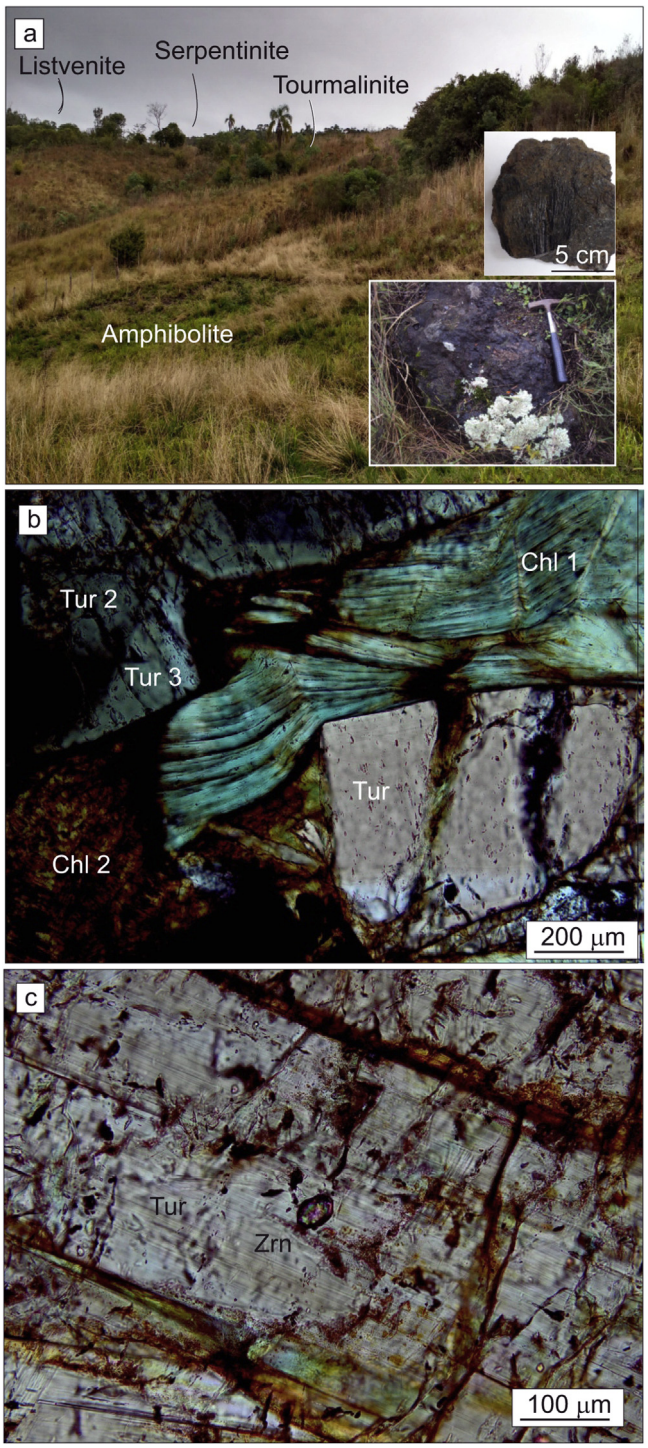

Figure 3. Photos of tourmalinite, Bossoroca ophiolite. (a) Field view, showing tourmalinite location surrounded by serpentinite (talc + olivine metaserpentinite) and associated oceanic crust rocks; insets show tourmalinite hand sample and outcrop; (b) Optical photomicrography (crossed nicols) showing low-amphibolite facies association of tur + chl 1 and greenschist facies chlo 2; tur 2 (dark core), 3 (light rim) apparent in upper left corner; tur unzoned in contact with chl 1, lower right corner; (c) Small (50 µm) zrn crystal included in tur; zrn size comparable to dated crystals.

Please cite this article as: Hartmann, L.A et al., Proto-Adamastor ocean crust (920 Ma) described in Brasiliano Orogen from coetaneous zircon and tourmaline, Geoscience Frontiers, https://doi.org/10.1016/j.gsf.2018.09.018

the same area of the crystal. Crystal number was kept the same for all analyses types. Mineral abbreviations follow Whitney and Evans (2010).

Three mounts were made of one section of tourmalinite to encompass the total length of tur crystals. Tourmaline was analyzed in the mounts with an electron microprobe for major elements and backscattered electron images, followed by boron isotope determinations with a laser. Chlorite associated to tourmaline was analyzed by EPMA, with BSE control. GCDKit freeware was used for plotting data in diagrams.

Detailed analytical procedures are described in Supplementary File 2, including zircon electron probe microanalyses, U-Pb-Hf isotopic and trace element determinations, and in tourmaline both major element and boron isotopic determinations.

4. Results

4.1. Field relations

The rounded, cubic block of massive tourmalinite is exposed 1 m on each side above the ground. The rock is dark nearly black, with large (1–10 cm) crystals of tourmaline (inset in Fig. 3a); minor chlorite is grey in color. The outcrop is barely visible under 1–2 m tall grass.

The tourmalinite is enclosed in metaserpentinite (Fig. 3a) with jackstraw arrangement of olivine and talc, plus minor opaque minerals. Olivine is altered to black serpentine and talc is gray, resulting in an easily identified texture in the field.

Amphibolite is associated with the serpentinite, and occurs mostly as loose blocks (10–50 cm in diameter) in the grasslands. The rock is medium-grained, dark colored (amphibole) with grey crystals (plagioclase). An unusual rock type near the tourmalinite is listvenite, that forms a massive exposure 50 m × 300 m, commonly bare rock 2–3 m above ground in the woods. The rock is grey, massive, with some chromite seams.

4.2. Sample and mineral description

The studied tourmalinite is massive, dark gray to black, and has minor zircon. Under the microscope, tourmaline is gray and only displays zoning in a narrow light rim (Fig. 3b). Intense cataclasis fractured and broke the crystals; vugs were generated during this process. Chlorite is present in two generations – Chl 1 in large crystals and Chl 2 in masses of small crystals, partly filling vugs (Fig. 3b). Chl 1

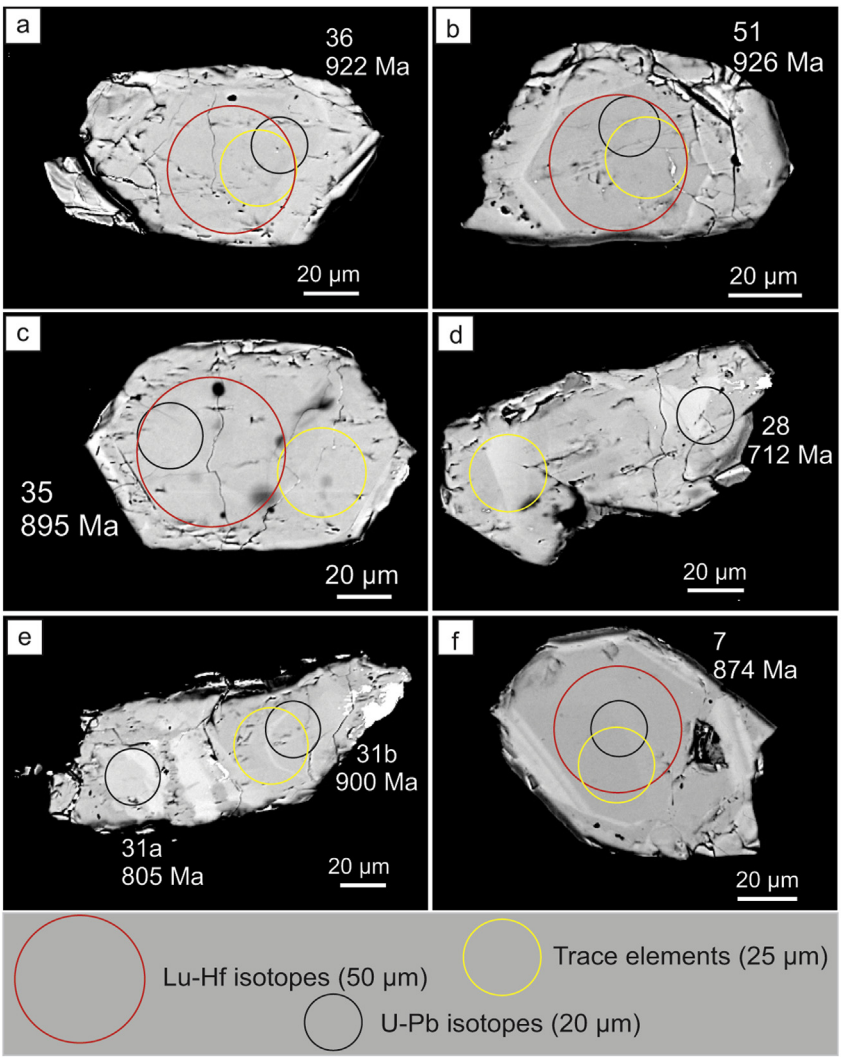

Figure 4. Selected BSE images of zircon, displaying location of spots analyzed for U-Pb-Hf and trace elements. (a–c) Concordant U-Pb ages; (d) Younger, discordant age caused by spot partly located over light gray new zircon; (e) Grain 31 displaying both concordant (31b) and discordant (31a) ages, discordance caused by spot location over partly recrystallized light grey zircon; (f) Younger, discordant age in homogeneous gray portion, discordance interpreted as Pb loss.

Please cite this article as: Hartmann, L.A et al., Proto-Adamastor ocean crust (920 Ma) described in Brasiliano Orogen from coetaneous zircon and tourmaline, Geoscience Frontiers, https://doi.org/10.1016/j.gsf.2018.09.018

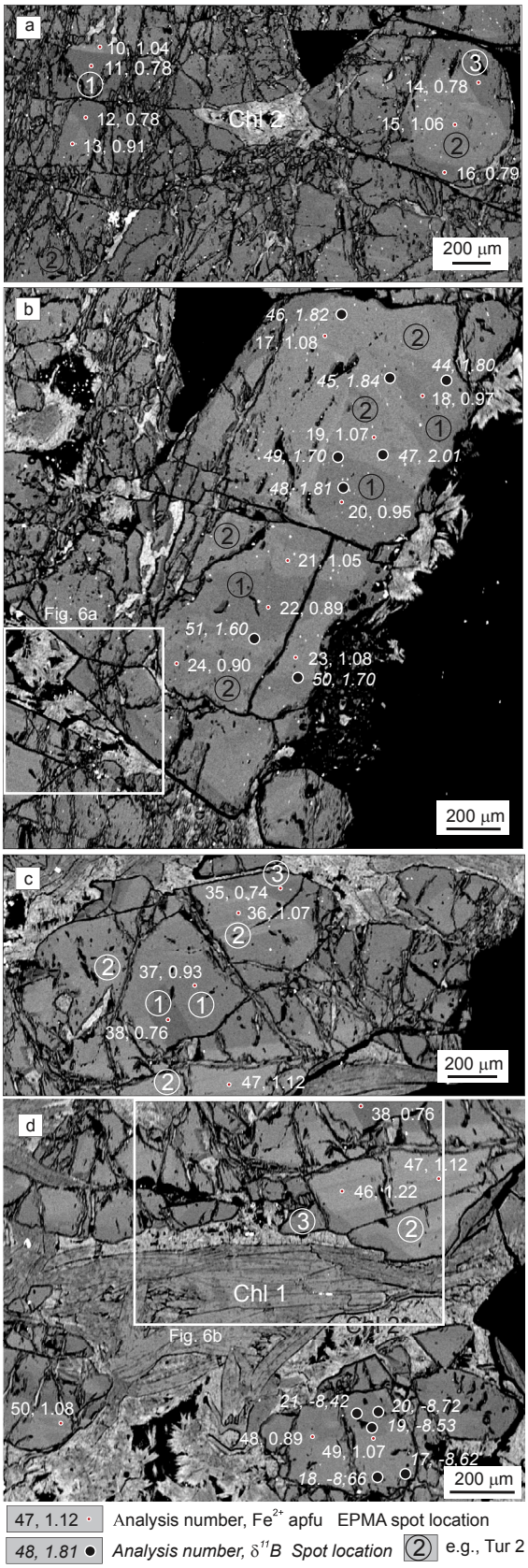

Figure 5. BSE images of tourmalinite. Different gray tones are tourmaline Tur 1, Tur 2, Tur 3 (circled numbers); Chl 1 is low amphibolite facies chlorite, Chl 2 is greenschist facies chlorite; location of spots for EPMA and $\delta^{11}B$ analyses indicated.

is in apparent equilibrium with tourmaline, but was deformed during cataclasis. Chl 2 seems in equilibrium with light tourmaline rim.

Zircon occurs included in tourmaline, mostly in strings of small (5–10 μm) crystals but reaching 50 μm (Fig. 3c), comparable in size to dated crystals. BSE imaging of 56 zircon crystals (six shown in Fig. 4) shows mostly anhedral shapes with some euhedral pyramids, aspect ratio 2:1 to 1:1, size 50–100 μm. A few fractures cross crystals but most are concentrated on rims. The main structure of the crystals is a large, homogenous core with few inclusions of euhedral apatite, surrounded by an irregular, fractured rim. The core (Zrn 1) is medium gray in BSE, whereas the rim (Zrn 2) has many light gray portions. The light gray, younger portions crosscut the medium gray core and similar medium gray rim, and were formed by fracture sealing (Hartmann et al., 1997). No euhedral zoning was observed. Rims are commonly porous, eventual mineral and fluid inclusions not determined.

Backscattered electron images (BSE) of tourmaline display internal structure including late cataclasis (Figs. 5 and 6). Three zones of different gray tones are observed in the images, although homogeneity is variable in each zone. Zones are preserved either at the core or along rims of crystal fragments (Fig. 7a). The better

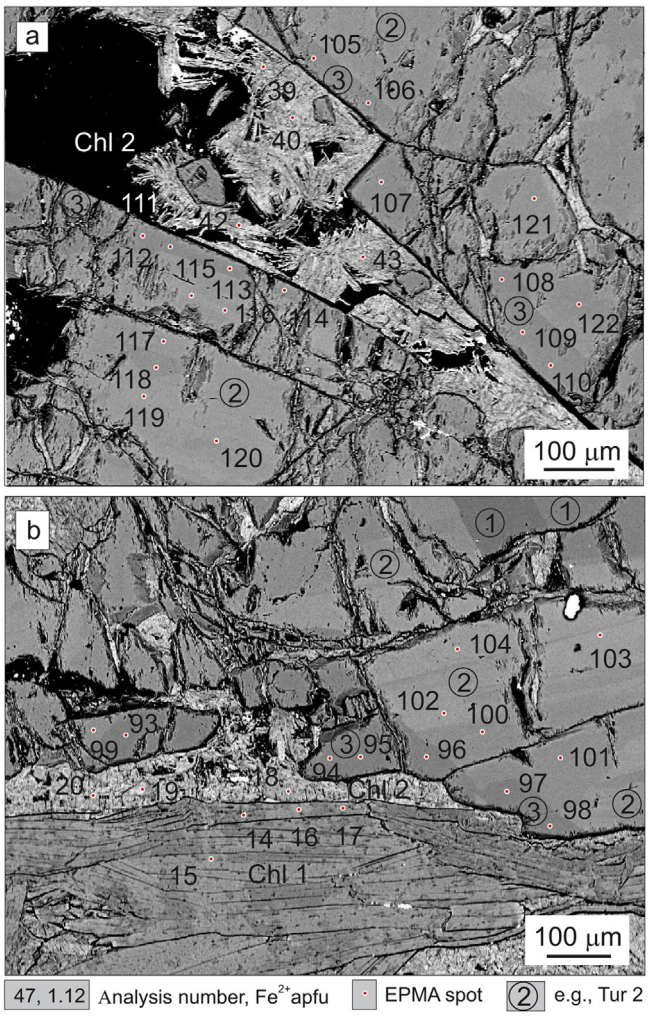

Figure 6. BSE images of tourmalinite. Different gray tones are tourmaline Tur 1, Tur 2, Tur 3 (circled numbers); Chl 1 is low amphibolite facies chlorite, Chl 2 is greenschist facies chlorite; red dots and numbers indicate position of EPMA analyses of tourmaline and chlorite.

Please cite this article as: Hartmann, L.A et al., Proto-Adamastor ocean crust (920 Ma) described in Brasiliano Orogen from coetaneous zircon and tourmaline, Geoscience Frontiers, https://doi.org/10.1016/j.gsf.2018.09.018

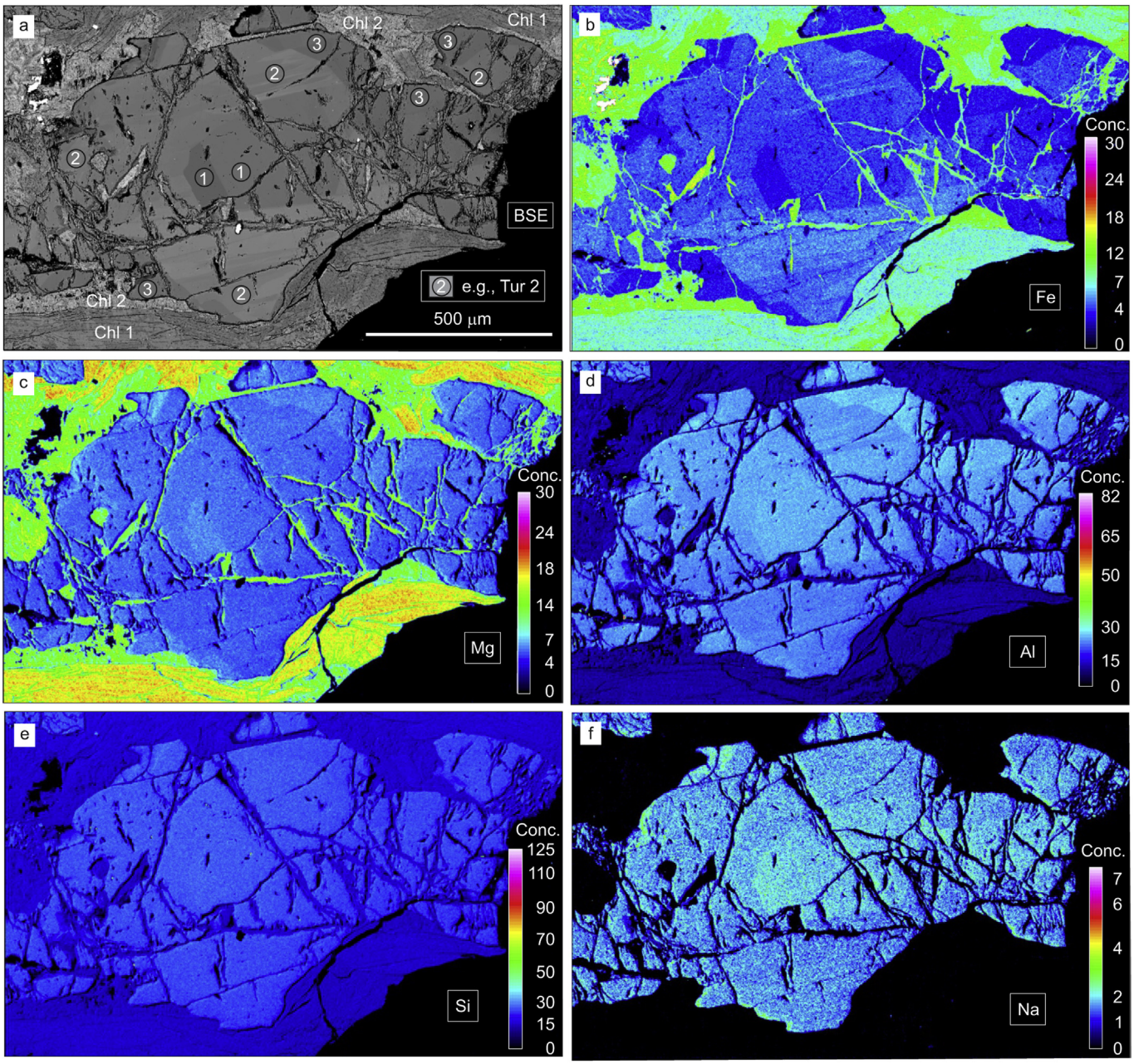

Figure 7. BSE and characteristic X-ray distribution of elements in tourmaline and chlorite. Tur 1, Tur 2, Tur 3 have different BSE intensities and different element concentrations except Si and Ca (not shown).

preserved, internal parts of crystals evidence a regular arrangement of two different zones (both included in Tur 1) as remnant, minor euhedral domains, bordered by Tur 2. Tur 1 has darkest in BSE core, succeeded by dark rim (Fig. 7a). Tur 2 is the lightest zone, homogeneous in a few portions but mostly intermingled with remnant Tur 1. Contacts between darker and less darker portions of Tur 1 are sharp, whereas Tur 2 is observed to cross Tur 1 in sub-micron heterogeneous portions. Tur 2 also displays two generations in BSE image (Fig. 7a), the younger discordant in relation to the older; nevertheless, we choose to include both in Tur 2. Tur 3 is present in dark rims in BSE on Tur 2 at the contact with Chl 2 but not at the contact with Chl 1.

The relationship between Chl 1 and Chl 2 is displayed in Figs. 3b and 5–7; larger (1 cm) crystals of Chl 1 are in contact with small (10 μm), fibrous crystals of Chl 2. Fibers extend into voids at the unfilled core of Chl 2 masses.

The integrated observation of BSE images and characteristic X-ray maps of tourmaline and chlorite (Fig. 7) displays several essential features. Tur 1, Tur 2, Tur 3 are observed in Fig. 7a, and these correspond to low Fe (wt.%) in Tur 1 and lowest Fe in Tur 3. Tur 2 has the highest Fe, heterogeneously distributed across Tur 1. Mg has complementary distribution to Fe. Al has high content in Tur 1, lowest in Tur 2 and highest in Tur 3. Si shows no variation for different zones, whereas Na (overall low) is higher in Tur 1 and lowest in Tur 2 and Tur 3. Ca content (not shown) is negligible.

The composition of chlorites is also shown in Fig. 7. In BSE image, Chl 2 is brighter than Chl 1. In compositional maps, Chl 2 has

Please cite this article as: Hartmann, L.A et al., Proto-Adamastor ocean crust (920 Ma) described in Brasiliano Orogen from coetaneous zircon and tourmaline, Geoscience Frontiers, https://doi.org/10.1016/j.gsf.2018.09.018

higher Fe (wt.%) than Chl 1 and complementary Mg content. Al and Si show no contrast between the two chlorites. Tur 3 rim has non-crystallographic, undulating contact with Tur 1 and Tur 2.

4.3. Zircon U-Pb-Hf isotopes and trace elements

We analyzed 29 spots in 26 zircon crystals for U-Pb isotopes, either one or two analyses per crystal (Supplementary File 3). The small size of homogeneous portions restricted the correct placement of the larger laser spot for Hf isotopic analyses in some crystals. Trace element analyses were mostly on homogenous, medium gray portions, although a few analyses covered mixed dark-light gray portions (Fig. 4d). U content of cores is 50–150 ppm in most analyses, with Th/U ratios near 0.8.

As exemplified in Fig. 4, homogenous cores yield concordant ages near 920 Ma (Fig. 8), but the intercept age is 920.4 ± 9.8 Ma, which we consider the age of crystallization of the core. Some grains show Pb-loss and yield 900, 890 and 870 Ma. Larger discordance is from mixed spots that covered mixed medium-light gray portions and yielded 805–712 Ma. Discordia line produces lower intercept without geological meaning. Selected grains are indicated in Figs. 4 and 8.

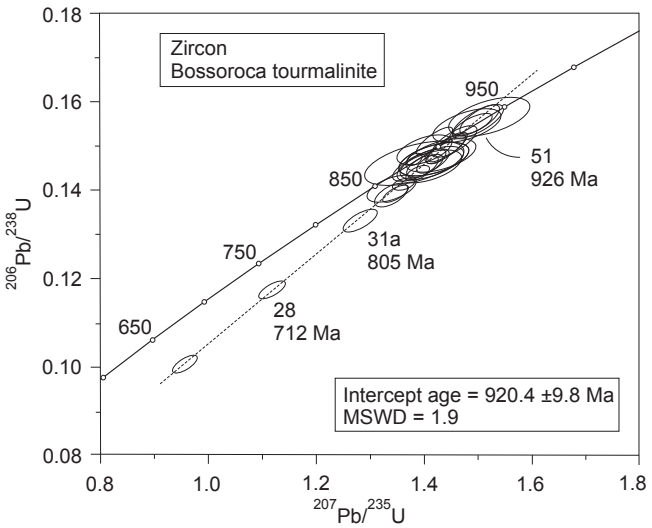

Figure 8. Concordia diagram displaying zircon isotopic determinations. A few selected grains indicated, with $^{206}Pb/^{238}U$ ages in Ma to display Pb loss during younger geological event.

Results of 16 analyses of Lu-Hf isotopes (Fig. 9; Supplementary File 4) are comparable to depleted mantle at 920 Ma, $\varepsilon_{Hf}(t) = +12$. Initial $^{176}Hf/^{177}Hf$ is close to 0.28255 without significant variation.

Trace element composition of zircon ($n = 33$ determinations (Fig. 10a–c; Supplementary File 5) indicates composition similar to derivation from depleted mantle (Grimes et al., 2015), common in zircon from oceanic crust (Fig. 10b). REE of studied zircon are similar to ophiolites in the Sul-Riograndense Shield (Fig. 10a; Arena et al., 2016, 2017, 2018a); positive Ce anomaly is accompanied by negative Eu anomaly. Composition is similar to MORB (Fig. 10c). Analyses in grains 15, 31, 53 resulted in higher REE than other grains; the spots were placed mostly over Zrn 1, but small (1 μm large) mineral inclusions and fractures were included in the spot.

4.4. EPMA analyses of tourmaline and chlorite

EPMA analyses display dravite compositions for all three zones and little variation in composition within each zone and overall (Fig. 12; Supplementary File 6). Composition ($n = 110$ analyses) is dominated by Si, Al, Fe, Mg, with low contents of Na and Ca. Fe^{3+}, Ti, Cr, Mn, K, F, Cl and Li contents are negligible.

Analyses ($n = 37$) of chlorite confirm the petrographic (Fig. 3b) and BSE (Figs. 6 and 7) observation of two generations, Chl 1 has low Fe, high Mg and Chl 2 has high Fe, low Mg (Supplementary File 7).

4.5. Boron isotopes of tourmaline

All three tourmaline zones (Tur 1, Tur 2, Tur 3) observed in BSE images and compositional maps find correspondence in $\delta^{11}B$ distribution (Fig. 11; Supplementary File 8). Based on 48 isotopic determinations, Tur 1 has $\delta^{11}B = +1‰$ to $+2.2‰$ (peak at $+1.8‰$), Tur 2 has $\delta^{11}B = -1‰$ to $+0.4‰$ (peak at $0‰$), Tur 3 has $\delta^{11}B = -8.2‰$ to $-9.2‰$, peak at $-8.5‰$). Compositional bimodality is suggested within different zones, but the gap is probably due to restricted number of analyses.

5. Interpretation

Chemical and isotopic data encoded in zircon and tourmaline from the Bossoroca tourmalinite are presently uncoded for delimitation of evolution of the minerals and host rocks. The Bossoroca ophiolite, as constrained by the study of rock association and minerals, is a fragment of Tonian lithosphere generated at the beginning of Rodinia fragmentation, proto-Adamastor Ocean.

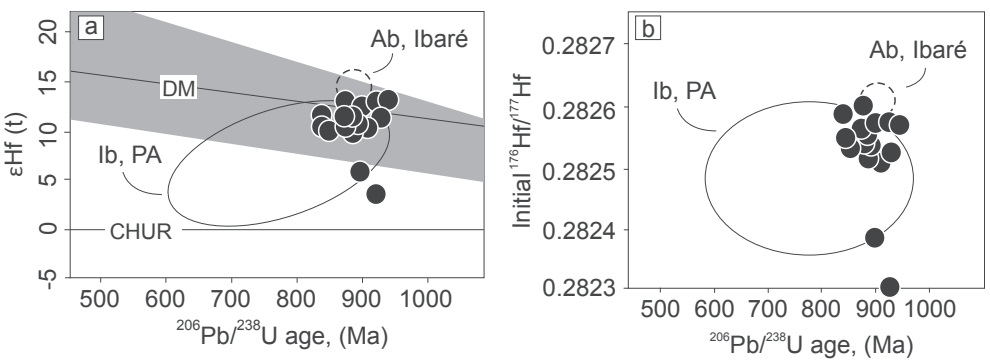

Figure 9. Hf isotopes of zircon vs. $^{206}Pb/^{238}U$ age. (a) $\varepsilon_{Hf}(t)$ close to +12, characteristic of derivation from depleted mantle. (b) $^{176}Hf/^{177}Hf_{(t)}$ similar to zircon from metasomatites, Ibaré and Palma ophiolites. DM = depleted mantle; CHUR = chondrite uniform reservoir. Highlighted field is depleted mantle evolution from Gerdes and Zeh (2006). Ib = Ibaré ophiolite, PA = Palma ophiolite, Ab = albitite.

Please cite this article as: Hartmann, L.A et al., Proto-Adamastor ocean crust (920 Ma) described in Brasiliano Orogen from coetaneous zircon and tourmaline, Geoscience Frontiers, https://doi.org/10.1016/j.gsf.2018.09.018

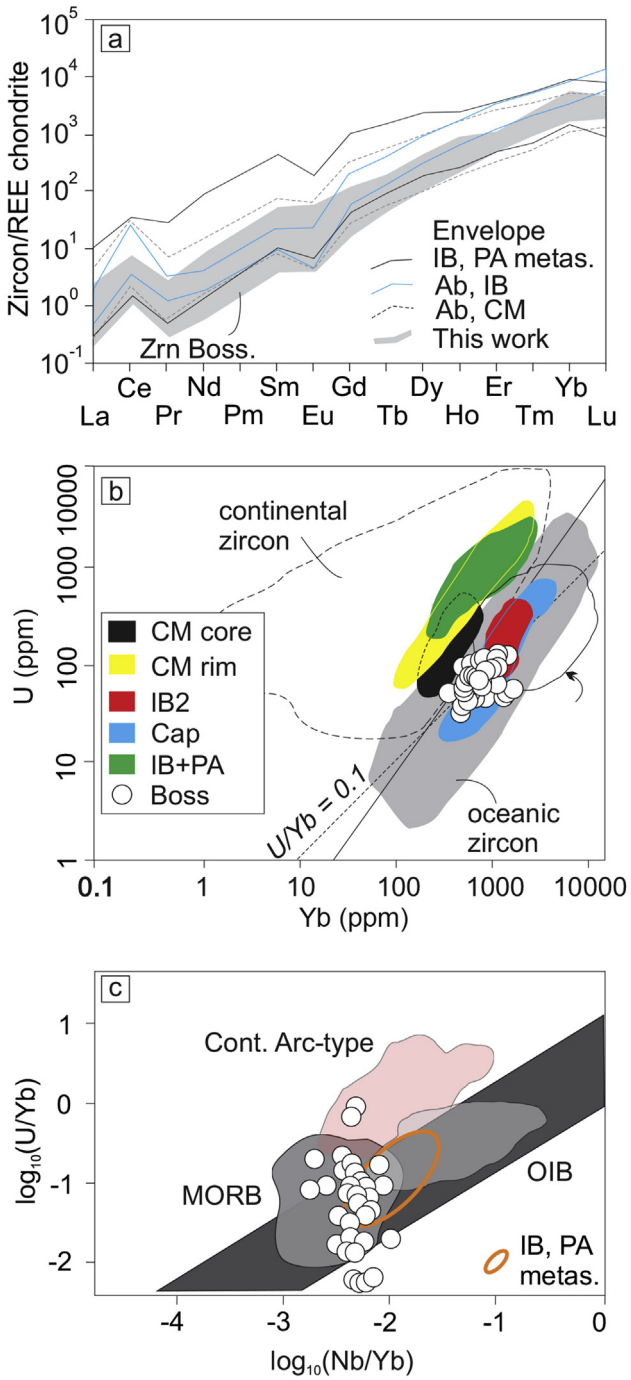

Figure 10. Trace-element composition of zircon from the Bossoroca tourmalinite. (a) REE diagram, normalized to Boynton (1984); envelopes of zircon composition from other ophiolites shown (IB, PA metas. = zrn from chloritite and tourmalinite, Ibaré and Palma; Ab, IB = albitite, Ibaré; Ab, CM = albitite, Cerro Mantiqueiras; Boss. = Bossoroca. (b) U versus Yb diagram (based on Grimes et al., 2007); studied Bossoroca zircon has oceanic crust composition. Known zircon compositions from ophiolites in the Sul-Riograndense Shield shown as colored fields (from Arena et al., 2016, 2017b); CM core = zrn core in albitite, Cerro Mantiqueiras, CM rim is the rim composition; IB2 = zrn in albitite, Ibaré; Cap = zrn in blackwall chloritite, Capané; IB + PA = zrn in chloritite and tourmalinite, Ibaré and Palma; Boss = zrn in tourmalinite, this work. Arrow indicates compositional field (circled by black line) of oceanic zircon from Araçuaí orogen (Schannor et al., 2018). (c) U/Yb versus Nb/Yb diagram displaying studied Bossoroca zircon with MORB composition; zircon composition from IB, PA (Ibaré, Palma) metasomatites from Arena et al. (2017) shown for comparison.

Interpretation of the data is significant for the evolution of the ophiolite and of the Brasiliano Orogen in the context of Rodinia.

Tourmaline - $(Ca, K, Na, [\ ])(Al, Fe, Li, Mg, Mn)_3(Al, Cr, Fe,V)_6(BO_3)_3(Si, Al, B)_6O_{18}(OH, F)_4$ is widespread in altered oceanic rocks mostly as disseminated crystals and rarely as massive tourmalinites (Slack and Trumbull, 2011), particularly in boron-rich mud volcanoes (Slack et al., 1998), thus becoming a key to the evolution of ophiolites. Tourmaline forms in all metamorphic grades from chlorite zone to upper amphibolite facies and occasionally granulite facies (Henry and Dutrow, 1996; Berryman et al., 2017), but tourmalinite evolution from altered oceanic crust and obduction onto a volcanic arc remains little known. Chemical and isotopic complexity and stability of the mineral to alteration in most geological processes are an asset to understand sequence of processes in evolving oceanic and continental crust. Tourmaline metamorphic and metasomatic crystallization is a response to several factors, mostly bulk composition of host rock, pressure, temperature and fluid composition (e.g., Ranta et al., 2017). Hydrothermal zircon contained in tourmalinite allows the determination of timing of oceanic crust alteration.

Zircon yielded the age of crystallization at 920.4 ± 9.8 Ma of large, homogeneous cores (Zrn 1), and displays the result of a younger event (Zrn 2) identified from other studies (e.g., Machado et al., 1990; Remus et al., 1999) at 750–700 Ma. This result acquires greater significance because $\varepsilon_{Hf(920\ Ma)} = +12$ and zircon geochemistry indicates derivation from depleted mantle (MORB) in the altered oceanic crust. Generally-accepted criteria are lacking for zircon characterization from hydrothermal environments (Kapyaho et al., 2017; Zhu et al., 2017). We interpret the origin of zircon as hydrothermal, because it occurs included in tourmaline, internal structure and chemical composition.

Tourmaline retains isotopic composition of its formation (e.g., Berryman et al., 2016), because of negligible diffusion and refractory nature (Van Hinsberg et al., 2011). The studied tourmalinite sample has variation of $\delta^{11}B$ and average + 1.8‰ (Tur 1) characteristics close to altered oceanic crust and specifically terrigenous marine sediments (Supplementary File 9). Oceanic crust and ocean water were considered the origin of positive boron isotopes in 3.5 Ga rocks by Farber et al. (2015). Hydrothermally altered basalts from the oceanic crust contain relatively constant $\delta^{11}B$ values (−0.1‰ to +1.0‰), as observed by Ishikawa and Nakamura (1992).

Internal homogeneity of the two sub-zones of Tur 1 is suggestive of direct growth from a large reservoir of constant composition, namely the proto-Adamastor Ocean. This is comparable to unzoned tourmaline described by Zhang et al. (2018). Heterogeneous internal structure of Tur 2 and its $\delta^{11}B$ peak at 0‰ are interpreted as isolation of Tur 1 from direct contact with ocean water; fluid infiltration altered partly Tur 1, originated in host terrigenous marine sediments. These continent-derived sediments were present in the initial rift of the proto-ocean.

Fluids from the continental crust commonly generate tourmaline with low $\delta^{11}B$ (e.g., Zheng et al., 2018). In the studied tourmaline (low $\delta^{11}B = -8.5$‰ in Tur 3), continental fluids reached the studied sample through fractures caused by faulting. Greenschist facies metamorphism altered partly the existent Chl 1 to form Chl 2 in vugs. Fluids extracted Fe from Tur 1 and Tur 2 to add to Chl 2, forming dark in BSE rims on the tourmaline. Fracturing of tourmaline continued in milder conditions, without reaction rims. Progressive metamorphism is expected to decrease $\delta^{11}B$ (Nakano and Nakamura, 2001), as presently observed.

Studied dravite has three different zones in BSE images, chemistry and $\delta^{11}B$. Intensity of electron back-scattering is linked to

Please cite this article as: Hartmann, L.A et al., Proto-Adamastor ocean crust (920 Ma) described in Brasiliano Orogen from coetaneous zircon and tourmaline, Geoscience Frontiers, https://doi.org/10.1016/j.gsf.2018.09.018

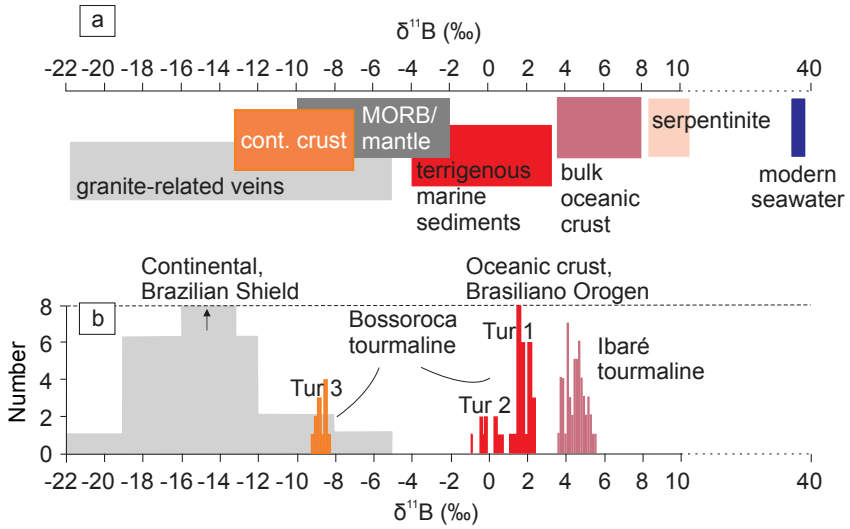

Figure 11. Boron isotopic composition of Bossoroca dravite and boron reservoirs. Field of selected continental crust (Archean and Neoproterozoic) of Brazilian Shield from Garda et al. (2009), Trumbull et al. (2013) and Albert et al. (2018). Brasiliano Orogen oceanic crust from Arena et al. (2018) and this work.

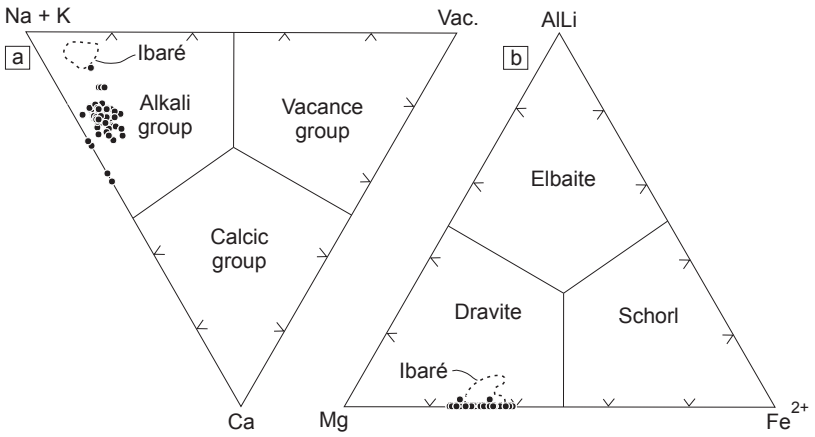

Figure 12. Triangular classification diagrams of Bossoroca tourmaline. Ibaré tourmaline (Arena et al., 2018b) shown for comparison.

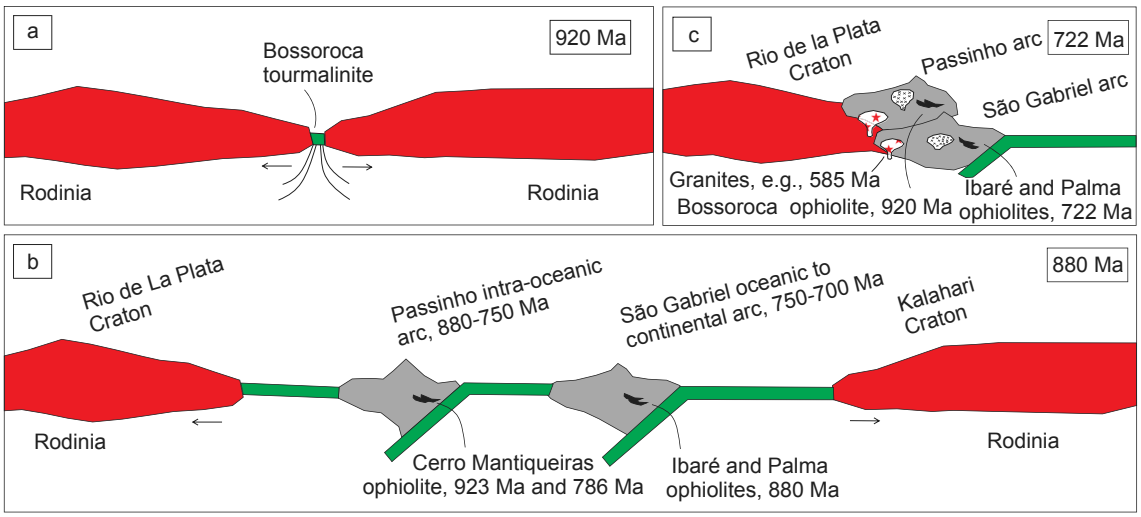

Figure 13. Evolutionary model of oceanic crust from initial rupturing of Rodinia (a) to sequential formation of oceanic arc (Passinho) and oceanic to continental arc (São Gabriel) (b) and final incorporation of the ophiolites to the margin of Rio de La Plata Craton (c). Proto-Adamastor Ocean formed at 920 Ma and evolved into a world-scale Adamastor Ocean in sequence. Bossoroca tourmalinite formed during initial oceanic crust formation, in a continentally-influenced environment of narrow-rift.

Please cite this article as: Hartmann, L.A et al., Proto-Adamastor ocean crust (920 Ma) described in Brasiliano Orogen from coetaneous zircon and tourmaline, Geoscience Frontiers, https://doi.org/10.1016/j.gsf.2018.09.018

average atomic number of cations per pixel and can be simplified by observation of distribution of Fe^{2+} apfu in different zones. Atomic number of Fe = 26, Mg = 12, Si = 14, Al = 13, Na = 11, Ca = 20. Darkest grey zone (Tur 1) is oldest and has lowest Fe^{2+} content (0.74–0.85 apfu), overgrown by light grey zone (Tur 2) that has high Fe^{2+} content (0.85–1.25 apfu). The youngest Tur 3 has also low Fe^{2+} content, similar to Tur 1. Mg apfu has inverse correlation with Fe^{2+} apfu, Si and Al also contribute to electron emission but without significant correlation with BSE signal. Na and Ca are low and make a small contribution. Similar control of electron backscattering control by Fe^{2+} apfu was found by Choo (2003).

The coetaneous evolution of zircon and tourmaline makes these observations most relevant, because both minerals are resilient to alteration by metamorphism. Their presence in one rock sample, zircon included in tourmaline, allows a test of relative resilience. The different zones in Tur 1, Tur 2, Tur 3 find no direct correspondence in internal structure of zircon. Only Zrn 1 and Zrn 2 were identified in BSE images as a homogeneous, large core, partly altered (mostly along fractures) into small, lighter gray portions. Only the cores were confidently dated at 920.4 ± 9.8 Ma, the rims too narrow for full spot location but suggesting ages near 700 Ma.

We correlate the homogeneous cores of zircon (Zrn 1) and tourmaline (Tur 1) as formed during the first crystallization event, in direct contact with proto-Adamastor Ocean water. Tur 1 formed thus at 920.4 ± 9.8 Ma. Partial recrystallization of both minerals, forming Zrn 2 and Tur 2, is understood as an oceanic-crust event within terrigenous marine sediments. The presence of significant marine deposits on either side of the present Atlantic Ocean (e.g., Basei et al., 2018) supports the presence of the deposits during initial proto-Adamastor Ocean. The negligible Fe^{3+} content points to oceanic, reducing environment. Restricted access of fluid and presumed lower temperature partly altered Zrn 1 into Zrn 2 and Tur 1 into Tur 2.

Thrusting of the ophiolite onto an oceanic arc caused intense deformation of the rocks, crystallization of Chl 2 and alteration of Tur 1 and Tur 2 into Tur 3 along rims originated from tourmaline fracturing. No discernible, coetaneous alteration of zircon with Tur 3 was identified. Either zircon is more resilient to alteration than tourmaline or zircon alteration related to the late fluids mingled with bright in BSE zones in Zrn 2 and remained undetermined.

The integrated, multi-proxy investigation of coetaneous zircon and tourmaline from a single sample seems a fertile method of characterization of oceanic crust and mantle in ophiolites. Their resilience is particularly useful, mostly the different resistance of the two minerals to alteration during same processes.

The Bossoroca ophiolite, and its contained tourmalinite, is a key rock association formed at the beginning of Rodinia rifting (Fig. 13a). Our focus on processes at 920 Ma is most significant (see also Arena et al., 2016, 2017), because Rodinia break-up and the consequent opening of major oceanic basins is commonly considered for a later period of 800–700 Ma (Oriolo et al., 2017).

Continued rifting into an active, small oceanic basin (Fig. 13b) developed a first oceanic arc (Passinho oceanic arc, 880–750 Ma) onto which the ophiolite was obducted. This is interpreted as corresponding to D2 thrusting (Saalmann et al., 2007). The wider Adamastor Ocean led to the formation of the São Gabriel arc (750–700 Ma), also containing ophiolites (Arena et al., 2016, 2017, 2018a). Age of formation of Zrn 2 needs additional studies, but several tectonic events occurred between 880 Ma and 700 Ma in the São Gabriel terrane (Arena et al., 2016, 2017, 2018a).

The ophiolite-containing arcs (Fig. 13c) later collided and overthrusted the Rio de La Plata Craton (a fragment of Rodinia) to build a significant configuration of the early Brasiliano Orogen. A testimony to the initial rifting of Rodinia was thus preserved. Coetaneous zircon and tourmaline provide evidence for crystallization at 920 Ma from a large oceanic reservoir in proto-Adamastor Ocean, followed by alteration caused by limited-volume fluids contained in rift-related, terrigenous marine sediments. After these oceanic processes, a collisional process overthrew the tourmalinite and containing ophiolite onto a craton, evidence encoded as negative $\delta^{11}B$ of tourmaline rims.

Rocks as rare as the studied massive tourmalinite are of major significance for the evolution of supercontinent and embayed oceanic crust, because they occur in particular oceanic rock associations (serpentinite, amphibolite, listvenite) and contain information on the coetaneous evolution of zircon and tourmaline. Multi-proxy investigations decode the characteristics of both minerals, U-Pb dating, depleted mantle composition, zoning, specific boron isotopes. Resilience to alteration is different for both minerals and can be compared. One additional, small point is established for the beginning rifting of Rodinia, located in the Sul-Riograndense Shield, Brasiliano Orogen.

6. Conclusions

Initial Rodinia rifting caused invasion of supercontinent new margins by Proto-Adamastor ocean and is registered in oceanic crust and mantle in Brasiliano Orogen. Integrated field (tourmalinite, serpentinite, amphibolite, listvenite), U-Pb-Hf zircon isotopes (920.4 ± 9.8 Ma, $\varepsilon_{Hf(920\ Ma)} = +12$) and elements (REE, 'oceanic' U-Yb, MORB composition), and dravite isotopes ($\delta^{11}B = +1.8‰, 0‰, -8.5‰$) led to the first identification of proto-Adamastor in the orogen, Bossoroca ophiolite. Characterization of evolution of coetaneous hydrothermal zircon and tourmaline in massive tourmalinite is a powerful tool for investigation of ophiolites and initial rifting of supercontinents.

Acknowledgements

We acknowledge field support from José Alírio Lenzi at Mina da Bossoroca. Conselho Nacional do Desenvolvimento Científico e Tecnológico (Government of Brazil) supported systematically investigations by the authors, including undergraduate scholarship to Mariana Werle. EPMA analyses were obtained from 'Laboratório de Microanálises do DEGEO/EM – Laboratório integrante da Rede de Microscopia e Microanálises de Minas Gerais – FAPEMIG'. We acknowledge the contributions of two anonymous referees to the qualification of the article.

Appendix A. Supplementary data

Supplementary data to this article can be found online at https://doi.org/10.1016/j.gsf.2018.09.018.

References

Albert, C., Lana, C., Gerdes, A., Schannor, M., Narduzzia, F., Queiroga, G., 2018. Archean magmatic-hydrothermal fluid evolution in the Quadrilátero Ferrífero (SE Brazil) documented by B isotopes (LA MC-ICPMS) in tourmaline. Chemical Geology 481, 95–109.

Arena, K.R., Hartmann, L.A., Lana, C., 2016. Evolution of Neoproterozoic ophiolites from the southern Brasiliano Orogen revealed by zircon U-Pb-Hf isotopes and geochemistry. Precambrian Research 285, 299–314.

Arena, K.R., Hartmann, L.A., Lana, C., 2017. Tonian emplacement of ophiolites in the southern Brasiliano Orogen delimited by U-Pb-Hf isotopes of zircon from metasomatites. Gondwana Research 49, 296–332.

Arena, K.R., Hartmann, L.A., Lana, C., 2018a. U-Pb-Hf isotopes and trace elements of metasomatic zircon delimit the evolution of the neoproterozoic Capané ophiolite in the southern Brasiliano Orogen. International Geology Review 60, 911–928.

Arena, K.R., Hartmann, L.A., Lana, C., Queiroga, G.N., Castro, M.P., 2018b. Geochemistry and $\delta^{11}B$ Evolution of Massive Tourmaline from the Tonian Ibaré

Ophiolite, Southern Brasiliano Orogen. Annals Brazilian Academy of Sciences (accepted for publication).
Basei, M.A.S., Frimmel, H.E., Campos Neto, M.C., Ganade de Araujo, C.E., Castro, N.A., Passarelli, C.R., 2018. The tectonic history of the southern Adamastor ocean based on a correlation of the Kaoko and Dom Feliciano belts. In: Siegesmund, S., et al. (Eds.), Geology of Southwest Gondwana, Regional Geology Reviews. Springer International Publishing AG, part of Springer Nature, pp. 63–85.
Berryman, E.J., Kutzschbach, M., Trumbull, R.B., Meixner, A., van Hinsberg, V., Kasemann, S.A., Franz, G., 2017. Tourmaline as a petrogenetic indicator in the pfitsch formation, western tauern window, eastern Alps. Lithos 284–285, 138–155.
Berryman, E.J., Wunder, B., Rhede, D., Schettler, G., Franz, G., Heinrich, W., 2016. P–T–X controls on Ca and Na distribution between Mg–Al tourmaline and fluid. Contributions to Mineralogy and Petrology 171 (31), 1–14.
Bogdanova, S.V., Pisarevsky, S.A., Li, Z.X., 2009. Assembly and breakup of Rodinia (some results of IGCP project 440). Stratigraphy and Geological Correlation 17, 259–274.
Boynton, W.V., 1984. Cosmochemistry of the rare earth elements; meteorite studies. In: Henderson, P. (Ed.), Rare Earth Element Geochemistry. Elsevier, pp. 63–114.
Brito-Neves, B.B., Campos Neto, M.C., Fuck, R.A., 1999. From Rodinia to western Gondwana: an approach to the Brasiliano-Pan African cycle and orogenic collage. Episodes 22, 155–166.
Cawood, P.A., Strachan, R.A., Pisarevsky, S.A., Gladkochub, D.P., Murphy, J.B., 2016. Linking collisional and accretionary orogens during Rodinia assembly and breakup: implications for models of supercontinent cycles. Earth and Planetary Science Letters 449, 118–126.
Choo, C.O., 2003. Mineralogical studies on complex zoned tourmaline in diaspore nodules from the Milyang clay deposit, Korea. Geosciences Journal 7, 151–156.
Farber, K., Dziggel, A., Trumbull, R.B., Meyer, F.M., Wiedenbeck, M., 2015. Tourmaline B-isotopes as tracers of fluid sources in silicified Palaeoarchaean oceanic crust of the Mendon Formation, Barberton greenstone belt, South Africa. Chemical Geology 417, 134–147.
Garda, G.M., Trumbull, R.B., Beljavskis, P., Wiedenbeck, M., 2009. Boron isotope composition of tourmalinite and vein tourmalines associated with gold mineralization, Serra do Itaberaba Group, central Ribeira Belt, SE Brazil. Chemical Geology 264, 207–220.
Gerdes, A., Zeh, A., 2006. Combined U-Pb and Hf isotope LA-(MC)-ICP-MS analyses of detrital zircons: comparison with SHRIMP and new constraints for the provenance and age of an Armorican metasediment in Central Germany. Earth and Planetary Science Letters 249, 47–61.
Grimes, C.B., John, B.E., Kelemen, P.B., Mazdab, F., Wooden, J.L., Cheadle, M.J., Hanghøj, K., Schwartz, J.J., 2007. The trace element chemistry of zircons from oceanic crust: a method for distinguishing detrital zircon provenance. Geology 35, 643–646.
Grimes, C.B., Wooden, J.L., Cheadle, M.J., John, B.E., 2015. "Fingerprinting" tectono-magmatic provenance using trace elements in igneous zircon. Contributions to Mineralogy and Petrology 170, 46.
Gubert, M.L., Philipp, R.P., Basei, M.A.S., 2016. The Bossoroca complex, São Gabriel terrane, Dom Feliciano belt, southernmost Brazil: U-Pb geochronology and tectonic implications for the neoproterozoic São Gabriel arc. Journal of South American Earth Sciences 70, 1–17.
Hartmann, L.A., Delgado, I.M., 2001. Cratons and orogenic belts of the Brazilian Shield and their contained gold deposits. Mineralium Deposita 36, 207–217.
Hartmann, L.A., Philipp, R.P., Santos, J.O.S., McNaughton, N.J., 2011. Time frame of 753-680 Ma juvenile accretion during the São Gabriel orogeny, southern Brazil. Gondwana Research 19, 84–99.
Hartmann, L.A., Takehara, L., Leite, J.A.D., McNaughton, N.J., Vasconcellos, M.A.Z., 1997. Fracture sealing in zircon as evaluated by electron microprobe analyses and back-scattered electron imaging. Chemical Geology 141, 67–72.
Henry, D.J., Dutrow, B.L., 1996. Metamorphic tourmaline and its petrologic applications. Reviews in Mineralogy 33, 503–557.
Ishikawa, T., Nakamura, E., 1992. Boron isotope geochemistry of the oceanic crust from DSDP/ODP Hole 504B. Geochimica et Cosmochimica Acta 56, 1633–1639.
Kapyaho, A., Molnar, F., Sorjonen-Ward, P., Manttari, I., Sakellaris, G., Whitehouse, M.J., 2017. New U-Pb age constraints for the timing of gold mineralization at the Pampalo gold deposit, Archaean Hattu schist belt, eastern Finland, obtained from hydrothermally altered and recrystallised zircon. Precambrian Research 289, 48–61.
Koppe, J.C., Hartmann, L.A., Lisboa, P.F.C., Monteiro, R.N., 1985. Aspectos geológicos e estratigráficos do Complexo Bossoroca, São Sepé, Rio Grande do Sul. In: Simp. Sul-brasil. Geol., vol. 2. SBG, Anais, Florianópolis, Brasil, pp. 32–36.
Koppe, J.C., Hartmann, L.A., 1990. Geochemistry of the Bossoroca greenstone belt. Southernmost Brazil. Geochimica Brasiliensis 2, 167–174.
Lena, L.O.F., Pimentel, M.M., Philipp, R.P., Armstrong, R., Sato, K., 2014. The evolution of the Neoproterozoic São Gabriel juvenile terrane, southern Brazil based on high spatial resolution U-Pb ages and ^{18}O data from detrital zircons. Precambrian Research 247, 126–138.
Li, Z.X., Bogdanova, S.V., Collins, A.S., Davidson, A., De Waele, B., Ernst, R.E., Fitzimons, I.C.W., Fuck, R.A., Gladkochum, D.P., Jacobs, J., Karlstrom, K.E., Lu, S., Natapov, L.M., Pease, V., Pisarevsky, S.A., Thrane, K., Vernikovsky, V., 2008. Assembly, configuration, and break-up history of Rodinia: a synthesis. Precambrian Research 160, 179–210.
Machado, N., Koppe, J.C., Hartmann, L.A., 1990. A late proterozoic U-Pb age for the Bossoroca belt, Rio Grande do Sul, Brazil. Journal of South American Earth Sciences 3, 87–90.
Nakano, T., Nakamura, E., 2001. Boron isotope geochemistry of metasedimentary rocks and tourmalines in a subduction zone metamorphic suite. Physics of the Earth and Planetary Interiors 127, 233–252.
Nance, R.D., Murphy, J.B., 2013. Origins of the supercontinent cycle. Geoscience Frontiers 4, 439–448.
Oriolo, S., Oyhantçabal, P., Wemmer, K., Siegesmund, S., 2017. Contemporaneous assembly of Western Gondwana and final Rodinia break-up: implications for the supercontinent cycle. Geoscience Frontiers 8, 1431–1445.
Pertille, J., Hartmann, L.A., Santos, J.O.S., McNaughton, N.J., Armstrong, R., 2018. Reconstructing the Cryogenian-Ediacaran evolution of the Porongos fold and thrust belt, southern Brasiliano Orogen, based on zircon U-Pb-Hf-O isotopes. International Geology Review 59, 1532–1560. https://doi.org/10.1080/00206814.2017.1285257.
Philipp, R.P., Pimentel, M.M., Basei, M.A.S., 2018. The tectonic evolution of the São Gabriel terrane, Dom Feliciano belt, southern Brazil: the closure of the Charrua ocean. In: Siegesmund, S., et al. (Eds.), Geology of Southwest Gondwana, Regional Geology Reviews. Springer International Publishing AG, part of Springer Nature, pp. 243–265.
Queiroga, G.N., Pedrosa-Soares, A.C., Noce, C.M., Alkmim, F.F., Pimentel, M.M., Dantas, E., Martins, M., Castañeda, C., Suita, M.T.F., Prichard, F., 2007. Age of the Ribeirão da Folha ophiolite, Araçuaí Orogen: the U-Pb zircon dating of a plagiogranite. Geonomos 15, 61–65.
Ramos, R.C., Koester, E., Porcher, C.C., 2018. Chemistry of chromites from Arroio Grande ophiolite (Dom Feliciano belt, Brazil) and their possible connection with the Nama Group (Namibia). Journal of South American Earth Sciences 80, 192–206. https://doi.org/10.1016/j.jsames.2017.09.032.
Ranta, J.-P., Hanski, E., Cook, N., Lahaye, Y., 2017. Source of boron in the Palokas gold deposit, northern Finland: evidence from boron isotopes and major element composition of tourmaline. Mineralium Deposita 52, 733–746.
Remus, M.V.D., McNaughton, N.J., Hartmann, L.A., Koppe, J.C., Fletcher, I.R., Groves, D.I., Pinto, V.M., 1999. Gold in the Neoproterozoic juvenile Bossoroca volcanic arc of southernmost Brazil: isotopic constraints on timing and sources. Journal of South American Earth Sciences 12, 349–366.
Saalmann, K., Remus, M.V.D., Hartmann, L.A., 2006. Tectonic evolution of the Neoproterozoic São Gabriel block, southern Brazil: constraints on Brasiliano orogenic evolution of the Rio de La Plata cratonic margin. Journal of South American Earth Sciences 21, 204–227.
Saalmann, K., Remus, M.V.D., Hartmann, L.A., 2007. Neoproterozoic magmatic arc assembly in the southern Brazilian Shield – constraints for a plate tectonic model for the Brasiliano orogeny. Geotectonic Research 95, 41–59.
Santos, J.O.S., Chernicoff, C.J., Zappettini, E.O., McNaughton, N.J., Hartmann, L.A., 2019. Large geographic and temporal extensions of the Río de La Plata Craton, South America, and its metacratonic eastern margin. International Geology Review 61, 56–85. https://doi.org/10.1080/00206814.2017.1405747.
Schannor, M., Lana, C., Fonseca, M.A., 2018. São Francisco - Congo craton break-up: insights from U-Pb-Hf and trace elements of zircons in metasediments of the Araçuaí orogen. Geoscience Frontiers. https://doi.org/10.1016/j.gsf.2018.02.011.
Slack, J.F., Trumbull, R.B., 2011. Tourmaline as a recorder of ore-forming processes. Elements 7, 321–326.
Slack, J.F., Turner, R.J.W., Ware, P.L.G., 1998. Boron-rich mud volcanoes of the Black Sea region: modern analogues to ancient sea-floor tourmalinites associated with Sullivan-type Pb-Zn deposits? Geology 26, 439–442.
Stern, R.J., 2018. Neoproterozoic formation and evolution of Eastern Desert continental crust – the importance of the infrastructure-superstructure transition. Journal of African Earth Sciences 146, 15–27. https://doi.org/10.1016/j.jafrearsci.2017.01.001.
Suita, M.T.F., Pedrosa-Soares, A.C., Leite, C.A.S., Nilson, A.A., Prichard, H.M., 2004. Complexos ofiolíticos do Brasil e a metalogenia comparada das faixas Araçuaí e Brasília. In: Pereira, E.S., Castroviejo, R., Ortiz, F. (Eds.), Complejos ofiolíticos em Ibero América: Edita Proyecto XIII.1, Madrid-España. 379, pp. 101–132.
Trumbull, R.B., Beurlen, H., Wiedenbeck, M., Soares, D.R., 2013. The diversity of B isotope variations in tourmaline from rare element pegmatites in the Borborema Province of Brazil. Chemical Geology 352, 47–62.
van Hinsberg, V.J., Henry, D.J., Marschall, H.R., 2011. Tourmaline: an ideal indicator of its host environment. The Canadian Mineralogist 49, 1–16.
Whitney, D.L., Evans, B.W., 2010. Abbreviations for names of rock-forming minerals. American Mineralogist 95, 185–187.
Zhang, W., Chen, H., Peng, L., Zhao, L., Huang, J., Lub, W., Liang, P., Lai, C., 2018. Discriminating hydrothermal fluid sources using tourmaline boron isotopes: example from Bailingshan Fe deposit in the Eastern Tianshan, NW China. Ore Geology Reviews 98, 28–37.
Zheng, Z., Chen, Y.-J., Deng, X.-H., Yue, S.-W., Chen, H.-J., Wang, Q.-F., 2018. Tourmaline geochemistry and boron isotopic variations as a guide to fluid evolution in the Qiman Tagh W–Sn belt, East Kunlun, China. Geoscience Frontiers. https://doi.org/10.1016/j.gsf.2018.04.007.
Zhu, M., Zhang, L., Dai, Y., Wang, C., Peng, Z., 2017. Hydrothermal modification of zircon geochemistry and Lu–Hf isotopes from the Hongtoushan Cu–Zn deposit, China. Ore Geology Reviews 86, 707–718.

Please cite this article as: Hartmann, L.A et al., Proto-Adamastor ocean crust (920 Ma) described in Brasiliano Orogen from coetaneous zircon and tourmaline, Geoscience Frontiers, https://doi.org/10.1016/j.gsf.2018.09.018